JCI The Journal of Clinical Investigation

AKT activation promotes PTEN hamartoma tumor syndrome–associated cataract development

Caterina Sellitto, … , Richard T. Mathias, Thomas W. White

J Clin Invest. 2013;123(12):5401-5409. https://doi.org/10.1172/JCI70437.

Research Article **Ophthalmology**

Mutations in the human phosphatase and tensin homolog (*PTEN*) gene cause PTEN hamartoma tumor syndrome (PHTS), which includes cataract development among its diverse clinical pathologies. Currently, it is not known whether cataract formation in PHTS patients is secondary to other systemic problems, or the result of the loss of a critical function of PTEN within the lens. We generated a mouse line with a lens-specific deletion of *Pten* (PTEN KO) and identified a regulatory function for PTEN in lens ion transport. Specific loss of PTEN in the lens resulted in cataract. PTEN KO lenses exhibited a progressive age-related increase in intracellular hydrostatic pressure, along with, increased intracellular sodium concentrations, and reduced Na^+/K^+-ATPase activity. Collectively, these defects lead to lens swelling, opacities and ultimately organ rupture. Activation of AKT was highly elevated in PTEN KO lenses compared to WT mice. Additionally, pharmacological inhibition of AKT restored normal Na^+/K^+-ATPase activity in primary cultured lens cells and reduced lens pressure in intact lenses from PTEN KO animals. These findings identify a direct role for PTEN in the regulation of lens ion transport through an AKT-dependent modulation of Na^+/K^+-ATPase activity, and provide a new animal model to investigate cataract development in PHTS patients.

AKT activation promotes PTEN hamartoma tumor syndrome–associated cataract development

Caterina Sellitto,[1] Leping Li,[1] Junyuan Gao,[1] Michael L. Robinson,[2] Richard Z. Lin,[1] Richard T. Mathias,[1] and Thomas W. White[1]

[1]Department of Physiology and Biophysics, Stony Brook University, Stony Brook, New York, USA.
[2]Department of Zoology, Miami University, Oxford, Ohio, USA.

Mutations in the human phosphatase and tensin homolog (*PTEN*) gene cause PTEN hamartoma tumor syndrome (PHTS), which includes cataract development among its diverse clinical pathologies. Currently, it is not known whether cataract formation in PHTS patients is secondary to other systemic problems, or the result of the loss of a critical function of PTEN within the lens. We generated a mouse line with a lens-specific deletion of *Pten* (PTEN KO) and identified a regulatory function for PTEN in lens ion transport. Specific loss of PTEN in the lens resulted in cataract. PTEN KO lenses exhibited a progressive age-related increase in intracellular hydrostatic pressure, along with, increased intracellular sodium concentrations, and reduced Na^+/K^+-ATPase activity. Collectively, these defects lead to lens swelling, opacities and ultimately organ rupture. Activation of AKT was highly elevated in PTEN KO lenses compared to WT mice. Additionally, pharmacological inhibition of AKT restored normal Na^+/K^+-ATPase activity in primary cultured lens cells and reduced lens pressure in intact lenses from PTEN KO animals. These findings identify a direct role for PTEN in the regulation of lens ion transport through an AKT-dependent modulation of Na^+/K^+-ATPase activity, and provide a new animal model to investigate cataract development in PHTS patients.

Introduction

Germline mutations in the human phosphatase and tensin homolog (*PTEN*) gene cause a collection of rare syndromes collectively known as PTEN hamartoma tumor syndrome (PHTS; ref. 1). The best-described syndrome within PHTS is Cowden's disease (2), where *PTEN* mutations have been identified in more than 80% of patients (1, 3). Clinical presentation of Cowden's disease is complex, like other PHTS disorders, and covers a broad spectrum of health problems that often involve cancer and include abnormalities of the eye in approximately 13% of cases (4). Lens cataract is a common pathology among Cowden's disease patients with ocular involvement, and germline *PTEN* mutations have been confirmed in PHTS cases in which cataract is present (3–7). Although global *Pten* deletion in mice is lethal (8), many tissue-specific KO models have been generated to examine the role of *Pten* mutation and/or deletion in different types of cancers linked to PHTS (1). In contrast, no animal models of lens cataract caused by *Pten* mutation have been described.

PTEN is a ubiquitously expressed dual-specificity enzyme that can act as either a lipid phosphatase that antagonizes class I PI3K signaling or as a protein phosphatase that can dephosphorylate serine and threonine residues (9, 10). Class I PI3Ks are lipid kinases acting downstream of cell surface receptors to phosphorylate the 3′-hydroxyl group of phosphatidylinositol-(4,5)P_2. The generated phosphatidylinositol-(3,4,5)P_3 (PIP_3) activates additional signaling pathways to regulate cell growth, proliferation, motility, and survival (11). One of the most well-characterized functions of PIP_3 is activation of the protein kinase AKT. PTEN dephosphorylates PIP_3 generated by PI3K and negatively regulates AKT activity (12, 13). The interplay among PTEN, PI3K, and AKT is central to the regulation of many cellular processes in a wide variety of tissues, including the ocular lens (14).

The crystallin lens is an avascular organ that is uniquely dependent on the activity of numerous membrane channels and transporters to maintain its transparency and prevent cataract (15). The human lens facilitates visual accommodation and contains a single layer of epithelial cells spanning the anterior half of its surface, differentiating fiber cells that constitute the cortex from mature fiber cells in the core that make up the most of the lens mass (14). The lens depends on ion transport to create an internal circulating current, with Na^+ being the primary current carrier (16). Na^+ enters the lens at the anterior and posterior poles and flows inward along the extracellular spaces. Within the lens, Na^+ is driven by its electrochemical gradient to move into the fiber cells, where the direction of flow is reversed and the current flows back to lens surface through gap junction channels (15, 17). Gap junction coupling is concentrated at the equator in peripheral fiber cells, directing the Na^+ current to the equatorial epithelium, where Na^+/K^+-ATPase activity pumps Na^+ out of the lens to complete the circulatory loop (18). Na^+ transport is coupled to fluid circulation, creating a microcirculatory system that carries nutrients to the fiber cells and allows removal of metabolic waste. The intracellular passage of fluid through gap junction channels is driven by a standing hydrostatic pressure gradient within the lens (19–21). The ensemble activity of the various membrane channels and transporters that drive this microcirculatory system overcomes the lack of a lens vasculature and supports clarity, consistent with the finding that mutations in many of these channel genes have been linked to congenital cataract (22).

PHTS encompasses a complex set of syndromic disorders that are united by their linkage to germline mutations within *PTEN*. As somatic mutations of *PTEN* are involved in many cancers, it is not

Conflict of interest: The authors have declared that no conflict of interest exists.
Citation for this article: *J Clin Invest.* 2013;123(12):5401–5409. doi:10.1172/JCI70437.

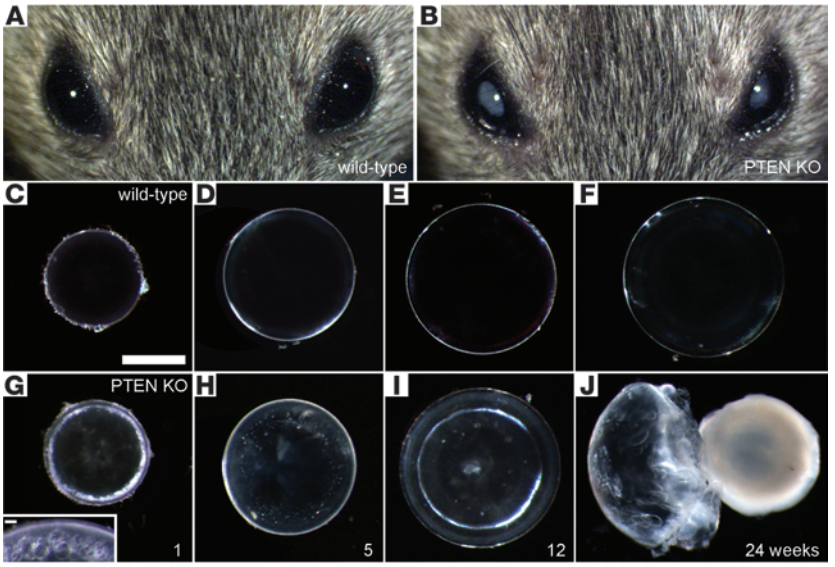

Figure 1
Lens-specific deletion of *Pten* causes cataract. (**A** and **B**) At 24 weeks of age, WT mice had clear eyes (**A**), while PTEN KO animals displayed obvious cataracts (**B**). (**C**–**F**) Dissected WT lenses remained transparent from 1 to 24 weeks. (**G**–**J**) PTEN KO lenses. At 1 week, PTEN KO animals had numerous cortical vacuoles (**G**, inset) that became punctate opacities by 5 weeks (**H**). At 12 weeks, PTEN KO lenses were noticeably larger than WT and showed varying degrees of opacity (**I**). By 24 weeks, the majority of PTEN KO lenses comprised a dense nuclear cataract and cortical lens fragments (**J**). Scale bars: 1 mm (**C**–**J**); 40 μm (**G**, inset).

surprising that an increased incidence of epithelial tumors (e.g., skin, colon, breast, thyroid, and endometrium) is found in PHTS patients (1, 3). The lens is unique among epithelial tissues in the body, as it is never spontaneously develops cancer (23). Thus, the cataract pathology in PHTS patients must arise from some activity of PTEN unrelated to cancer. To elucidate the mechanisms whereby *PTEN* mutation contributes to the loss of lens homeostasis and cataract, we generated and characterized a conditional KO mouse that lacks *Pten* in the lens. Our findings showed that PTEN plays an important role in the regulation of lens ion transport and that cataract in PHTS patients may result from increased AKT-dependent downregulation of Na^+/K^+-ATPase activity.

Results

Lens-specific Pten deletion causes cataract and lens rupture. Germline mutations in *PTEN* cause PHTS, which can include cataract (5, 6) as a clinical consequence. Whole-animal KO of *Pten* resulted in embryonic lethality (8), necessitating the generation of a lens-specific conditional KO to investigate the mechanism whereby cataracts are caused by *Pten* mutation. To achieve this, mice with a floxed *Pten* allele (24) were interbred with MLR10-*Cre* transgenic mice (25) to obtain lens-specific conditional KO mice (referred to herein as PTEN KO). MLR10-*Cre* mice utilize a modified αA-crystallin promoter containing a Pax6 consensus binding site to specifically express *Cre* recombinase in both the lens epithelium and fiber cells. Compared with littermate WT controls (i.e., floxed *Pten* animals without the MLR10-*Cre* transgene), cataracts were obvious in the intact eyes of adult PTEN KO mice at 24 weeks (Figure 1, A and B). Lenses isolated from WT mice remained transparent at all ages examined (Figure 1, C–F). In contrast, lenses dissected between 1 and 24 weeks of age from PTEN KO animals showed a progressive pathology. At 1 week, PTEN KO lenses exhibited a ring of densely packed cortical vacuoles (Figure 1G) that by 5 weeks had condensed into smaller opacities dispersed throughout the outer lens (Figure 1H). At 12 weeks, PTEN KO lenses were larger than WT lenses and had variable degrees of opacification (Figure 1I). Between 12 and 24 weeks, lenses became more opaque and began to rupture, ultimately leaving behind cortical fragments and a dense nuclear cataract (Figure 1J). These observations confirmed a specific role for PTEN in the maintenance of lens clarity and validated the PTEN KO model as a tool with which to discern the molecular mechanism of cataract in PHTS patients.

Changes in animal, eye, and lens size were quantified over time by dissecting and weighing eyes from age-matched PTEN KO and littermate WT mice. Lenses were dissected and photographed at 1, 2, 3, 5, 12, and 24 weeks of age, and their diameters were measured and subsequently used to calculate volumes, assuming spherical geometry. There was no significant difference in overall body size between WT and PTEN KO animals between 1 and 24 weeks (Figure 2A). However, changes in ocular mass were noted in adult mice, with PTEN KO eyes weighing 13% more than WT controls at 12 weeks, increasing to 19% greater PTEN KO eye mass at 24 weeks (Figure 2B). The effect of the PTEN KO phenotype on lens size also developed slowly, with a modest 2%–7% increase in lens volume between 1 and 5 weeks that grew to a 16% increase by 12 weeks and a 29% increase at 24 weeks, in the reduced number of intact lenses found at that age (Figure 2C). We also recorded the frequency of lens rupture between 1 and 24 weeks for WT and PTEN KO littermate animals. WT lenses never exhibited lens rupture in the time period examined, while 9.3% of PTEN lenses had ruptured at 12 weeks, increasing to an 81% incidence of rupture by 24 weeks (Figure 2D). These data suggested that PTEN regulates lens homeostasis, possibly by altering the activities of channels and transporters that control solute concentrations within the lens, ultimately causing lens and eye swelling and lens rupture.

PTEN KO produces a progressive increase in lens intracellular hydrostatic pressure. The lens depends on the coordinated activity of different channels and transporters to create a circulating current, with Na^+ being the primary current carrier (16, 17). The transport of Na^+ is coupled to circulation of fluid, and the intracellular passage of fluid through gap junction channels is driven by a hydrostatic pressure gradient (19–21). If the normal lens circulation was altered in PTEN KO animals, a buildup of osmotically active solutes within the lens could increase intracellular pressure at the lens surface, leading to the observed rupture phenotype. We previously developed a technique for directly measuring hydrostatic pressure in the lens (19, 26) and used this method here to determine whether progression of the PTEN KO phenotype correlated

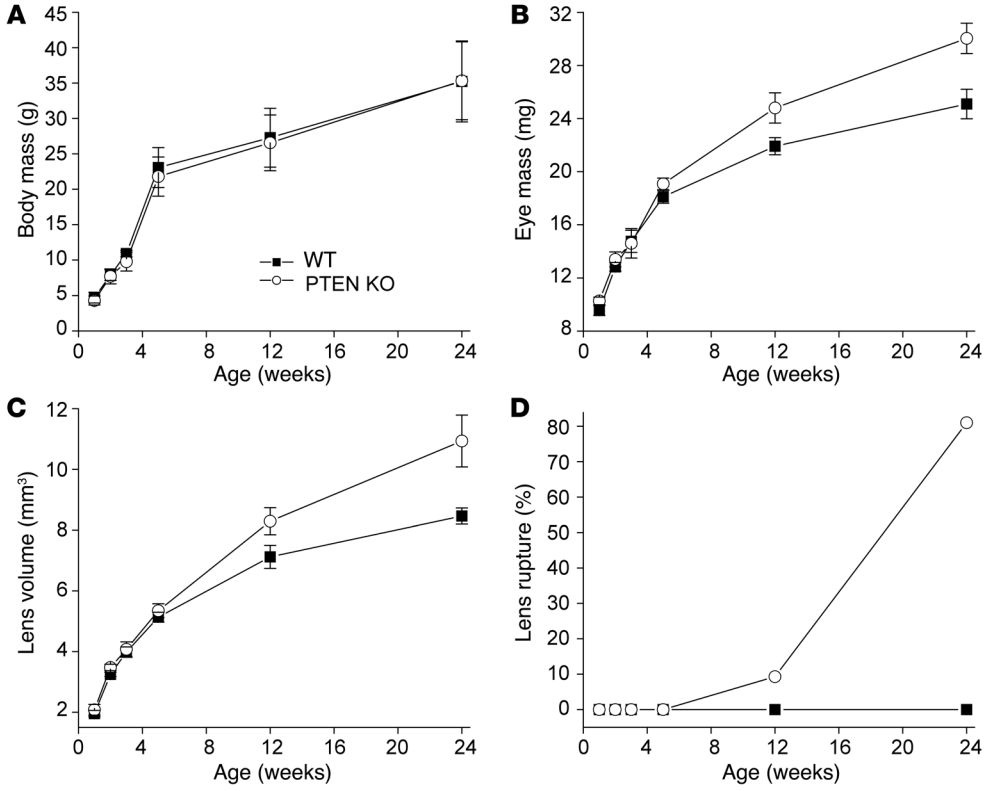

Figure 2
PTEN KO lenses display increased organ size and rupture. (**A**) There were no significant differences in overall body size between WT and PTEN KO mice at any age ($P > 0.05$, Student's *t* test). (**B**) Eye mass increased 13% at 12 weeks and 19% at 24 weeks in PTEN KO versus WT animals ($P < 0.05$). (**C**) PTEN KO mice had lenses that were 16% larger than WT at 12 weeks of age, which increased to 29% larger at 24 weeks ($P < 0.05$). (**D**) Whereas WT lenses never ruptured, 9.3% ($n = 43$) of PTEN KO lenses had ruptured at 12 weeks, and 81% ($n = 36$) had ruptured by 24 weeks. Data are mean ± SD. $n = 6–27$ per genotype per time point.

with changes in lens intracellular pressure (Figure 3). To derive quantitative values for the central and surface pressures, pooled data were graphed as a function of normalized distance from the lens center, then fit with an equation based on lens structure and experimentally derived transport parameters of the lens (19). At 6 weeks of age, there was extensive overlap between the pressure data derived from WT and PTEN KO lenses (Figure 3A). However, pressure values from PTEN KO lenses were consistently higher than those of WT littermate controls by 8 weeks (Figure 3B), and this difference increased further at the 10-week time point (Figure 3C). Best fit values for hydrostatic pressures at the WT lens surface and center were 0 ± 0 and 336 ± 16 mm Hg, respectively (mean ± SD), with minimal changes between 6 and 10 weeks of age. These data were in excellent agreement with our previously published studies of mouse lens intracellular pressure (19, 26) and confirmed the existence of a standing hydrostatic pressure gradient in the normal lens. In contrast, intracellular hydrostatic pressure in surface cells of the lens increased from 0 to 52 mm Hg between 6 and 10 weeks in PTEN KO mice (Figure 3D). This observation provides a molecular explanation of the cataractous rupture phenotype in PTEN KO mice. In previously studied lenses from various ages and different species, the hydrostatic pressure in lens surface cells was always equal to the pressure in the surrounding bathing solution (26). The increase in surface cell hydrostatic pressure in PTEN KO lenses is the most likely cause of rupture of the capsule and underlying cells. Central pressure in PTEN KO lenses also increased from 354 to 486 mm Hg during this time period (Figure 3E), although this would not be expected to cause lens rupture by itself, as modulation of gap junctional coupling can give rise to elevated central hydrostatic pressures, with normal surface pressures and no lens rupture (19). These data showed a strong temporal correlation between elevation of lens surface intracellular hydrostatic pressure and development of the rupture phenotype in PTEN KO lenses.

PTEN KO increases lens intracellular sodium concentration. Sodium transport drives lens circulation, and the intracellular hydrostatic pressure gradient is dependent on Na^+ concentration (16, 19). The elevation of central and surface hydrostatic pressure in PTEN KO lenses suggested that sodium transport may be compromised, and that Na^+ may be accumulating within cells. To test this, we used the Na^+ indicator dye SBFI to measure intracellular sodium concentrations in lenses of 10-week-old WT and PTEN KO mice (Figure 4). A SBFI-containing microelectrode was inserted into the lens near the surface, where the first SBFI injection was made. After diffusion of the dye into a fiber cell, fluorescence emission was recorded using 360- and 380-nm excitation wavelengths. The microelectrode was then advanced further into the lens, and additional injections and fluorescence measurements were made (Figure 4A). Data from several WT and PTEN KO lenses were pooled, and the 360/380 fluorescence emission ratios were calculated and plotted as a function of normalized distance from the lens center (Figure 4B). Depth-dependent calibration curves (27, 28) were then used to convert emission ratios to estimates of the internal Na^+ concentration at different positions within WT and PTEN KO lenses (Figure 4C). The dashed lines in Figure 4C show fits of the Na^+ concentration data to a previously described intracellular diffusion model (28). The best fit value for Na^+ concentration in WT lenses showed a gradient that varied from 14.6 mM at the lens center to 4.4 mM at the lens surface (Figure 4C), consistent with prior measurements in normal mouse lenses (27). In PTEN KO lenses, the gradient had noticeably shifted to higher lens Na^+ concentrations, with fitted values of 20.4 mM at the center and 7.9 mM at the surface (Figure 4C). Thus, the PTEN KO phenotype caused elevated intracellular

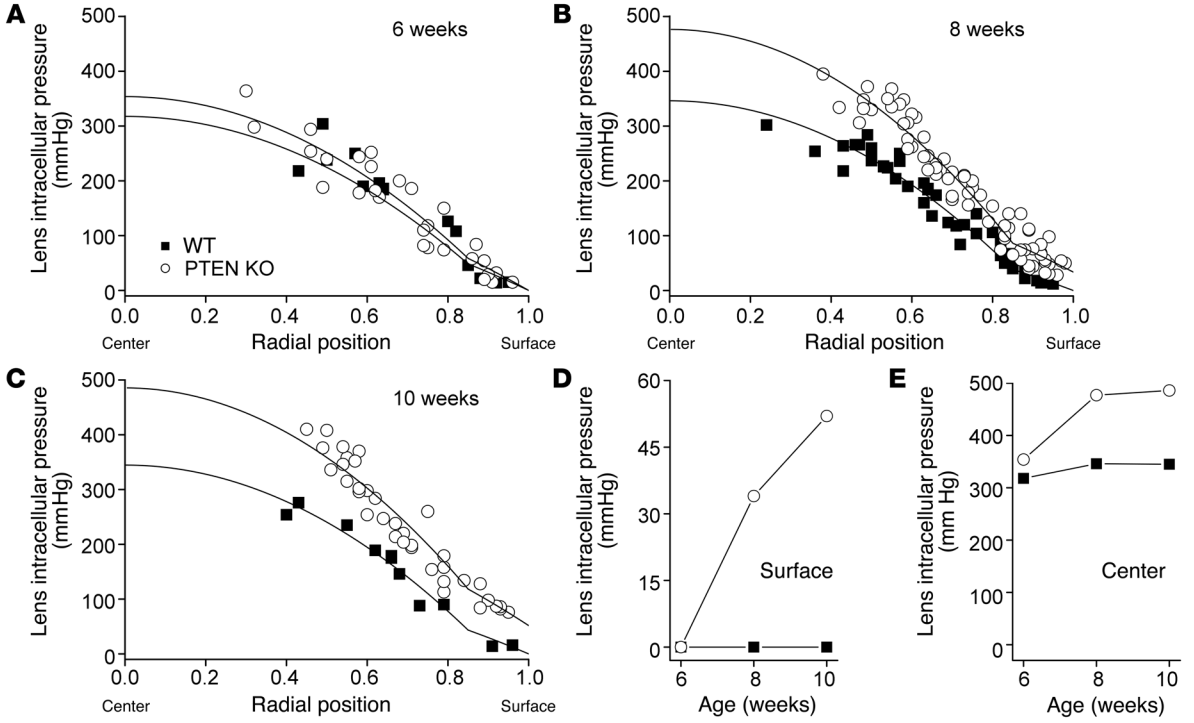

Figure 3

Lens hydrostatic pressure increases in PTEN KO mice. (**A**) At 6 weeks of age, pressure measurements from WT and PTEN KO lenses overlapped extensively. (**B**) At 8 weeks, however, pressure values from PTEN KO lenses were consistently higher than WT littermates. (**C**) In 10-week-old animals, pressure differences increased further. (**D** and **E**) Lens surface pressure increased from 0 to 52 mm Hg (**D**), and lens central pressure increased from 354 to 486 mm Hg (**E**), between weeks 6 and 10 in PTEN KO mice. *n* = 4–12 (WT) and 8–20 (PTEN KO) lenses per time point.

sodium, which may have increased the osmolarity of surface cells and induced elevated hydrostatic pressure to drive the circulating fluid out of the epithelium.

Na^+/K^+-ATPase activity is regulated by AKT and reduced in PTEN KO lens epithelial cells. The sodium current normally exits the lens through the equatorial epithelium, where Na^+/K^+-ATPase activity is concentrated (18). The increased Na^+ concentration measured within PTEN KO lenses may have resulted from a decrease in Na^+/K^+-ATPase activity, which in turn could be mediated by elevated PI3K signaling following *Pten* deletion. To investigate this possibility, we isolated lens epithelial cells from WT and PTEN KO mice and directly measured the Na^+/K^+-ATPase current in the presence or absence of an AKT inhibitor (Figure 5). The Na^+/K^+-ATPase current was measured by perfusion of individual lens epithelial cells under voltage clamp with the reversible inhibitor strophanthidin (Figure 5A). After determination of cell capacitance, Na^+/K^+-ATPase current densities were plotted for WT and PTEN KO epithelial cells (Figure 5B). Na^+/K^+-ATPase current density in WT epithelial cells was 0.69 ± 0.08 pA/pF (mean ± SD; n = 10). In PTEN KO epithelial cells, current density was significantly reduced to 0.33 ± 0.03 pA/pF ($P < 0.05$; n = 18). Incubation of PTEN KO epithelial cells with an AKT inhibitor for 30 minutes prior to Na^+/K^+-ATPase current measurement restored the mean current density to 0.66 ± 0.10 pA/pF ($P > 0.05$; n = 9), indistinguishable from that of WT cells. To determine whether Na^+/K^+-ATPase protein levels were altered and confirm that PI3K signaling was elevated in PTEN KO lenses, epithelial cell extracts were probed by Western blot (Figure 5C). WT epithelial cells expressed PTEN, which was completely absent from PTEN KO mice. When blots were probed with an antibody against the α subunit of the Na^+/K^+-ATPase, both WT and PTEN KO epithelial cells had bands of equal intensity. To ensure equivalent loading, blots were probed with a β-actin antibody, which was also present at equivalent levels in epithelial cells from WT and PTEN KO animals (Figure 5C). Thus, the reduction of Na^+/K^+-ATPase activity following *Pten* deletion was not due to reduced levels of Na^+/K^+-ATPase protein. Consistent with PTEN's antagonistic role toward PI3K signaling, levels of phospho-AKT were highly elevated in PTEN KO versus WT epithelial cells (Figure 5C). This elevation was completely reversed in PTEN KO epithelial cells by preincubation with an AKT inhibitor that has been previously shown to inhibit both AKT activity and phospho-AKT (29). Total AKT levels were not affected by PTEN KO in the presence or absence of the AKT inhibitor. Quantitation of band densities showed no significant differences in levels of β-actin or the Na^+/K^+-ATPase α subunit between WT and PTEN KO epithelial cells with and without AKT inhibition ($P > 0.05$; Figure 5D). In contrast, the phospho-AKT/total AKT ratio was elevated more than 10-fold in PTEN KO epithelial cells ($P < 0.05$) and significantly reduced by AKT inhibitor treatment (Figure 5D). Taken together, these data suggest that the loss of PTEN antagonism of PI3K activity resulted in elevated levels of phospho-AKT, which in turn produced an approximately 50% reduction in Na^+/K^+-ATPase activity in lens epithelial cells.

Na^+/K^+-ATPase activity modulates intracellular hydrostatic pressure in the intact lens. If downregulation of the Na^+/K^+-ATPase by AKT underlies the phenotype in PTEN KO lenses, then modulation of Na^+/K^+-

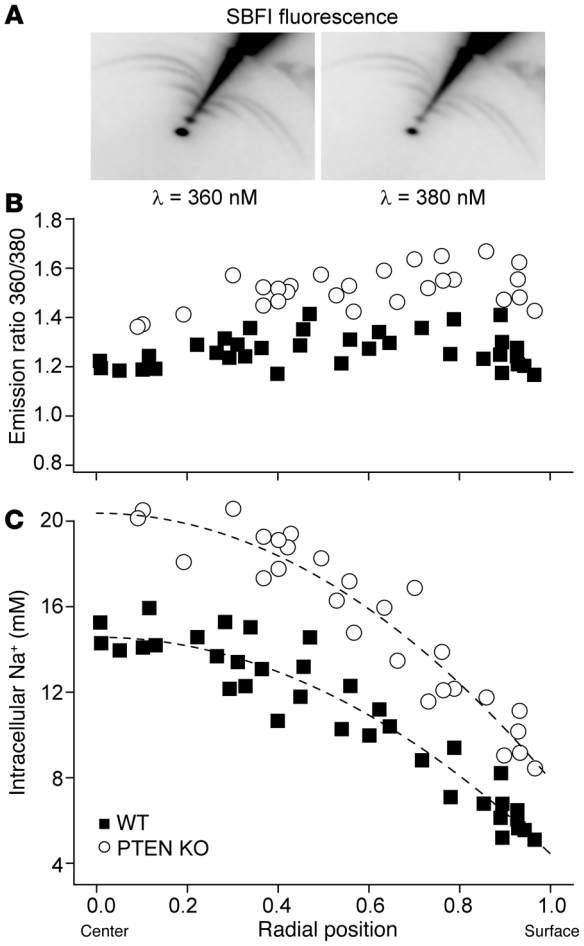

Figure 4
Increased lens intracellular sodium in PTEN KO mice. (**A**) Microelectrodes containing the sodium-sensitive dye SBFI were used to make a series of injections into lens fiber cells at different depths, and fluorescence emission was recorded using 360- and 380-nm excitation wavelengths. (**B**) 360/380 fluorescence emission ratios from lenses of 10-week-old WT and PTEN KO animals, plotted as a function of normalized radial distance from the lens center. (**C**) Emission ratios were converted to internal Na^+ concentrations and plotted against radial distance. Fits of the data (dashed lines) showed a Na^+ concentration gradient in WT lenses of 14.6 mM at the lens center to 4.4 mM at the lens surface. PTEN KO lenses had higher Na^+ concentrations, with fitted values of 20.4 mM at the center and 7.9 mM at the surface. Pooled data were obtained from 6 animals per genotype.

ATPase activity should alter intracellular hydrostatic pressure in the intact ex vivo lens. To examine this prospect, freshly dissected WT and PTEN KO lenses were impaled with pressure-sensing electrodes near the surface (at a radial position of 0.92 ± 0.02; mean ± SD) and perfused with strophanthidin and/or AKT inhibitor while intracellular pressure was continuously monitored (Figure 6). The initial pressure in WT lenses was 15.0 ± 1.0 mm Hg (n = 5), and this value remained stable for 20 minutes until the perfusion solution was changed to strophanthidin, which caused the pressure to rise to a new steady-state value of approximately 38.2 ± 1.2 mm Hg (P < 0.05; Figure 6A). As expected, PTEN KO lenses initially had an elevated pressure of 42.2 ± 1.6 mm Hg (n = 6), which dropped to a new steady-state value of 17.3 ± 0.8 mm Hg after perfusion with the AKT inhibitor (P < 0.05; Figure 6B). To confirm that these drugs were regulating the same process, we sequentially perfused PTEN KO lenses with the AKT inhibitor followed by strophanthidin (Figure 6C). The initial pressure in these lenses was also elevated, at 42.0 ± 2.0 mm Hg (n = 3), and dropped to 18.7 ± 1.2 mm Hg after AKT inhibitor perfusion. This new level of pressure remained stable for 20 minutes, then strophanthidin was added to the perfusion solution, and the pressure returned to ≥90% of its initial value over the next 80 minutes (38.0 ± 4.0 mm Hg; Figure 6C). These data showed that direct inhibition of Na^+/K^+-ATPase significantly increased lens hydrostatic pressure in WT lenses and that inhibition of AKT reduced pressure in PTEN KO lenses via AKT-dependent downregulation of Na^+/K^+-ATPase activity.

PTEN KO produces histological abnormalities in the equatorial region of the lens. If the improperly regulated Na^+/K^+-ATPase activity in the equatorial epithelium is responsible for the elevated Na^+ concentration and hydrostatic pressure in PTEN KO lenses, then osmotic damage would be expected to be occurring in this region of the lens (30). Dissection of 1-week-old intact lenses showed equatorial abnormalities consistent with this idea (Figure 1G). To look for histological defects in PTEN KO lenses, we dissected eyes from littermate mouse pups during the first postnatal week, sectioned them, and stained them with H&E (Figure 7). On P0, sagittal sections through the central region of WT lenses showed a normal appearance, while PTEN KO lenses displayed small vacuoles in the equatorial cortex beneath the ciliary body (Figure 7, A and B). Coronal sections of lenses at P2 confirmed that the vacuoles were absent from WT animals and were uniformly distributed across the equatorial region in PTEN KO eyes (Figure 7, C and D). Higher-magnification views of sagittal sections from P7 mice showed the normal differentiation of lens fibers from equatorial epithelial cells in WT lenses (Figure 7E). In PTEN KO lenses, epithelia-to-fiber differentiation also appeared to proceed normally at P7; however, numerous small vacuoles were present immediately underneath the equatorial epithelium (Figure 7F). Thus, the PTEN KO phenotype showed histological defects consistent with disruption of normal ion transport.

To test whether suppression of AKT activity could reduce vacuole formation in neonatal PTEN KO lenses, pregnant females were injected with vehicle or an AKT inhibitor once daily for the last 3 days of gestation (31). Lenses were dissected from pups at birth, fixed, sectioned, and stained with H&E (Supplemental Figure 1; supplemental material available online with this article; doi:10.1172/JCI70437DS1). Newborn PTEN KO lenses from vehicle-injected mothers developed extensive equatorial vacuoles, as expected (n = 8). In contrast, lenses of PTEN KO neonates from AKT inhibitor–treated mothers either displayed a substantial reduction in vacuole formation (56%; n = 9) or developed vacuoles to a similar extent as vehicle-treated controls (44%; n = 7). Combined with the ex vivo lens data in Figure 6, these results suggest that pharmacological inhibition of AKT can ameliorate many of the phenotypic defects underlying cataract formation and lens rupture following *Pten* deletion in mice.

Discussion

In hereditary syndromic disorders like PHTS, it can be difficult to determine whether the development of cataract in some patients is secondary to other widespread systemic abnormalities, or a pri-

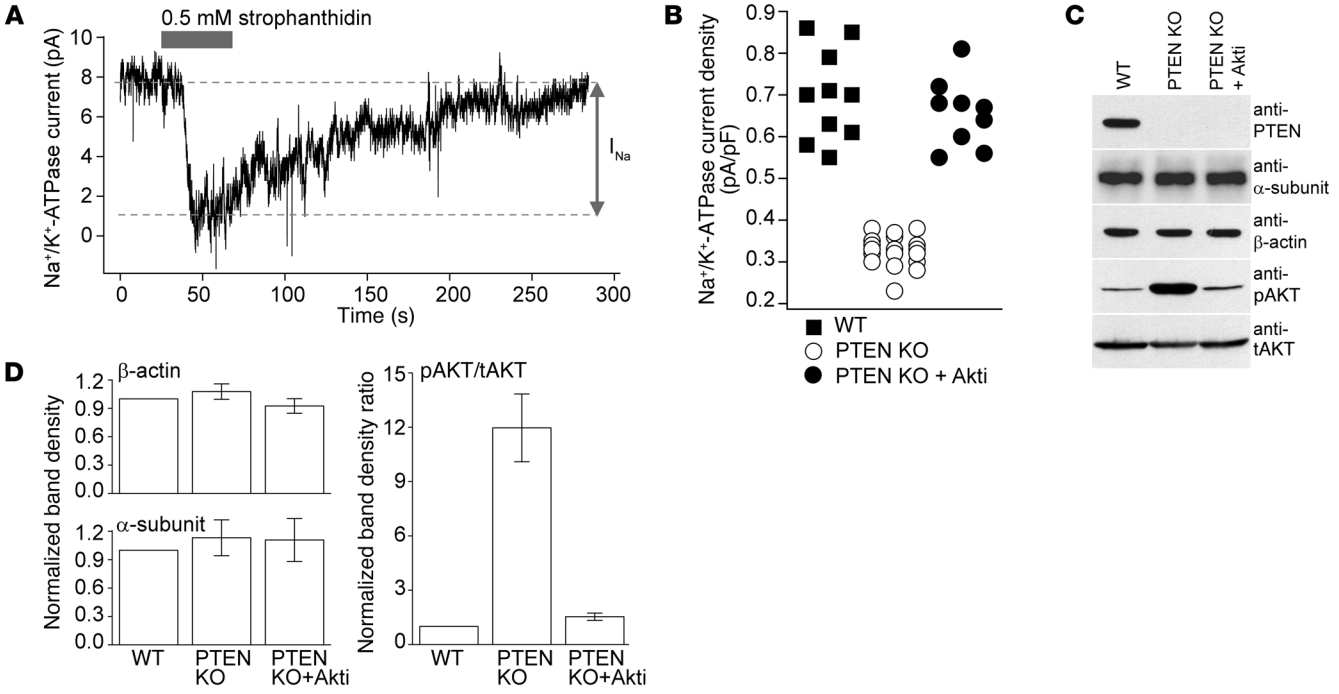

Figure 5

PTEN KO lens cells have decreased Na^+/K^+-ATPase activity caused by elevated phospho-AKT levels. (**A**) Na^+/K^+-ATPase current was measured by perfusion of lens epithelial cells under voltage clamp with strophanthidin. (**B**) Currents were divided by cell capacitance and plotted. WT cells had a Na^+/K^+-ATPase current density of 0.69 ± 0.08 pA/pF (n = 10). PTEN KO cell current density was reduced to 0.33 ± 0.03 pA/pF ($P < 0.05$; n = 18), which was restored to 0.66 ± 0.10 pA/pF (n = 9) by 30 minutes of preincubation with an AKT inhibitor (Akti). (**C**) Western blotting showed elevated PI3K signaling in PTEN KO lenses. WT lens epithelial cells expressed PTEN, which was absent from PTEN KO mice. The Na^+/K^+-ATPase α subunit was present at similar levels in WT and PTEN KO epithelial cells. Equivalent levels of β-actin were detected in epithelial cells from all animals. Phospho-AKT (pAKT) levels were elevated in PTEN KO epithelial cells, which could be reversed by preincubation with the AKT inhibitor. Total AKT (tAKT) levels were not affected by *Pten* deletion in the presence or absence of the AKT inhibitor. (**D**) Independent blots were quantitated and plotted (n = 4). Levels of β-actin and the Na^+/K^+-ATPase α subunit were not significantly different ($P > 0.05$). The phospho-AKT/total AKT ratio was elevated ≥10-fold in PTEN KO epithelial cells. Data (mean ± SD) were derived from 10-week-old mice.

mary consequence of lost function within the lens of the mutated causative gene. By generating a tissue-specific KO mouse lacking *Pten* only within the ocular lens, we identified a novel function for PTEN in the regulation of lens ion transport and homeostasis. Our PTEN KO animals displayed a cataractous rupture phenotype that developed over the first 6 months of life. PTEN KO lenses exhibited a progressive increase in hydrostatic pressure that correlated with increased intracellular sodium concentration and decreased Na^+/K^+-ATPase activity, leading to lens swelling, opacities, and ultimately organ rupture. AKT was highly activated in PTEN KO lenses, and pharmacological inhibition of AKT restored Na^+/K^+-ATPase activity to normal levels in primary cultured lens cells from PTEN KO animals, in addition to reducing pressure in intact PTEN KO lenses. These data confirmed a specific role for PTEN in the maintenance of lens clarity and provided a new animal model with which to investigate cataract development in PHTS patients.

Our PTEN KO mice gradually developed cataract between birth and 6 months of age. In Cowden's disease patients with *PTEN* mutations, cataract is often diagnosed between childhood and middle age. In one case report, the patient was in good health up to the age of 16 years, when he presented with initial symptoms that included blurred vision, and underwent cataract surgery at age 28 (6). In a second case, a male child presenting with PHTS features was found to have cataract at 6 years of age, which was then corrected surgically (5). We also found highly elevated levels of activated AKT in PTEN KO mice that were correlated with inhibition of lens Na^+/K^+-ATPase activity and elevated lens pressure. Although the status of lens AKT activity in Cowden's disease patients with cataract has not been described, it is interesting to note that patients with Proteus syndrome, another highly variable overgrowth syndrome caused by activating mutations in *AKT1* (32), also can develop childhood cataract (33). Thus, there is good congruence between our PTEN KO mouse model and forms of human syndromic cataract that involve inactivating mutations in *PTEN* or activating mutations in *AKT1*. These observations argue that PTEN, PI3K, and AKT play direct roles in the maintenance of lens clarity and that cataract in PHTS and other overgrowth syndromes is likely a primary pathology, not a secondary consequence of other systemic defects.

Our working hypothesis is that the loss of PTEN antagonism of PI3K signaling in the lens activates AKT, resulting in a reduction of Na^+/K^+-ATPase activity in equatorial epithelial cells. Sodium and water are then retained within lens cells, leading to increased intracellular hydrostatic pressure and ultimately lens cataract and rupture. Thus, perturbation of the balance among PTEN, PI3K, and AKT disrupted the lens circulation, which depends on the coordi-

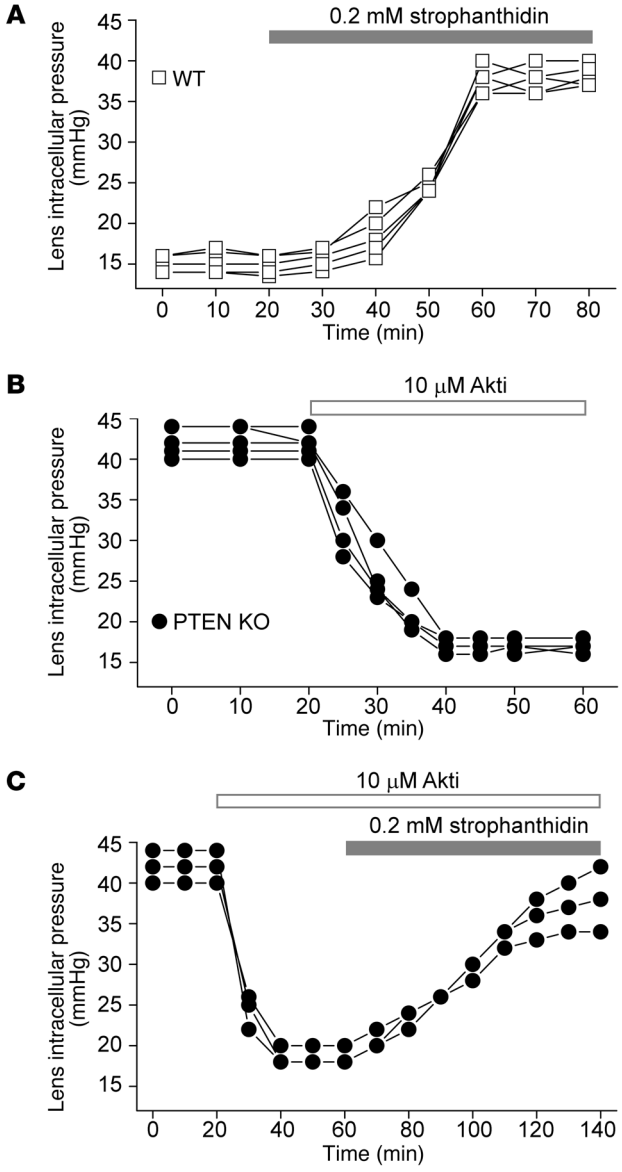

Figure 6
Lens hydrostatic pressure is modulated by Na^+/K^+-ATPase activity. (**A**) Intracellular pressure in WT lenses increased 2.5-fold after perfusion with strophanthidin (n = 5). (**B**) Pressure in PTEN KO lenses dropped 2.4-fold after perfusion with the AKT inhibitor (n = 6). (**C**) Perfusion of PTEN KO lenses with the AKT inhibitor resulted in a 2.2-fold decrease in lens pressure, which nearly recovered to the initial value by sequential perfusion with strophanthidin (n = 3). Data were derived from 10-week-old mice.

nated activity of many channels and transporters to maintain lens clarity. The importance of signal transduction pathways in regulating ion transport to establish and maintain the lens circulation has been previously highlighted by studies of lens connexin channels. Like Na^+/K^+-ATPase activity, connexin activity must be maximal in the equatorial region of the lens, and it has been shown that both FGF and bone morphogenetic protein (BMP) signaling pathways may help establish the gradient in connexin activity required for the lens circulation (34, 35). Similar to PTEN KO mice, constitutive activation in the lens of the MAP kinase signaling pathway downstream of the FGF receptor resulted in a cataractous rupture phenotype that was alleviated by specific deletion of the lens connexin target of MAP kinase (36). Na^+/K^+-ATPase activity is also known to be dynamically regulated in the lens (37, 38) and has been previously shown to respond to either purinergic or endothelin-1 receptor activation through the activity of Src family tyrosine kinases (39, 40). Our study expands the repertoire of Na^+/K^+-ATPase regulatory pathways in the lens to include PTEN, PI3K, and AKT.

One early manifestation of the PTEN KO phenotype was formation of a ring of densely packed cortical vacuoles in neonatal mice (Figure 1G) that preceded the elevation of lens hydrostatic pressure in adult animals by several weeks. Treatment in utero with an AKT inhibitor greatly reduced, or eliminated, vacuole formation in 54% of PTEN KO neonatal lenses (Supplemental Figure 1), which suggests that, like the hydrostatic pressure increase, this was also an AKT-dependent phenomenon. We have not measured the lens surface pressure in lenses of newborn PTEN KO mice and are uncertain how vacuole formation is related to the hydrostatic pressure changes linked to Na^+/K^+-ATPase activity in adult lenses. In addition, while there was good agreement between our pharmacological manipulation of Na^+/K^+-ATPase activity in isolated epithelial cells and hydrostatic pressure in intact lenses (Figures 5 and 6), the histological damage phenotype was more pronounced in the cortical fiber cells than in the epithelium itself. One possibility is that signaling regulated by PTEN could affect additional channels and transporters that contribute to the lens circulation — such as the connexins or aquaporins (15, 17), which are highly expressed in the cortical lens fibers — and that these proteins also contribute to changes in lens pressure and fiber cell morphology. Regardless of the precise mechanism of vacuole formation, our data suggest that pharmacological interventions based on AKT inhibition may show promise for alleviating some of the ocular manifestations of PHTS.

PTEN/PI3K regulation of ionic activity may be a general homeostatic mechanism that is perturbed in other disease states in addition to cataract. For example, it was recently shown that downregulation of PI3K signaling prolonged the QT interval of the cardiac action potential by affecting multiple ion channels, providing a possible mechanism to explain why some tyrosine kinase inhibitors in clinical use as anticancer therapies are associated with increased risk of arrhythmias like long QT syndrome (41, 42). In the central nervous system, PTEN regulation of synaptic transmission may help to explain abnormal social and cognitive behaviors observed in humans with PHTS and other neurological syndromes, such as autism spectrum disorders (43, 44). In the present study, we have shown that syndromic cataract linked to *PTEN* mutations could result from downregulation of the Na^+/K^+-ATPase in lens epithelial cells. Taken together, these observations suggest that PTEN, PI3K, and AKT may participate in regulation of the activity of diverse channels and transporters in many tissues, and that loss of this regulation may contribute to various disease states.

Methods

Generation of PTEN KO mice. *Pten* homozygous floxed mice (24) were interbred with MLR10-*Cre* mice (25) to obtain PTEN KO mice, with lens-specific conditional KO of *Pten*. Genotypes were verified by PCR of genomic tail DNA using sense (5′-CTCCTCTACTCCATTCTTCCC-3′) and antisense (5′-ACTCCCAC-CAATGAACAAAC-3′) primers to detect the floxed *Pten* allele. The MLR10-*Cre* transgene was amplified as previously described (25, 45).

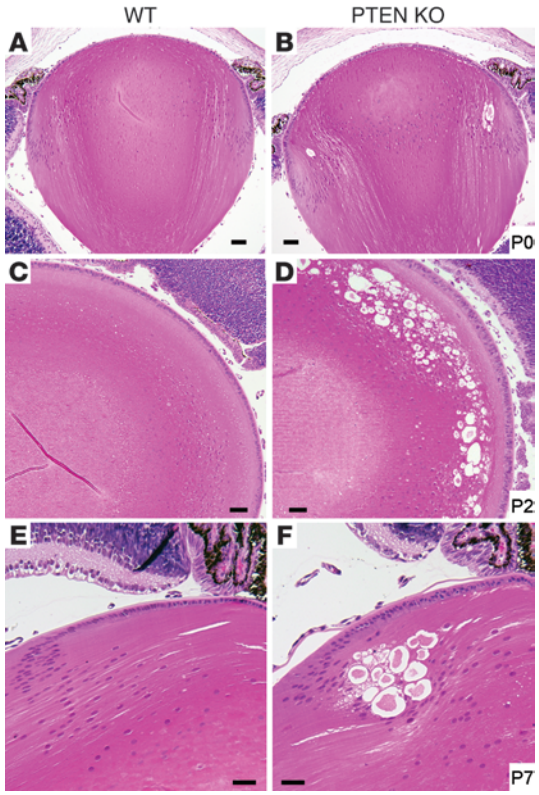

Figure 7
Histological abnormalities in PTEN KO lenses. (**A**) At P0, sagittal sections through the central region of WT lenses showed a normal appearance. (**B**) P0 PTEN KO lenses displayed small vacuoles in the equatorial cortex. (**C** and **D**) Coronal sections of P2 lenses confirmed the absence of vacuoles in WT animals (**C**), which were uniformly distributed across the equatorial region in PTEN KO mice (**D**). (**E**) Sagittal sections from P7 WT lenses showed normal differentiation of lens fibers from equatorial epithelial cells. (**F**) P7 PTEN KO lenses also showed normal fiber differentiation, in addition to numerous vacuoles immediately underneath the equatorial epithelium. Scale bars: 50 μm.

Growth analysis and lens photography. Age-matched littermate animals were weighed. Their eyes were dissected, weighed, and transferred to a Petri dish containing 37°C Tyrode solution on a warm stage. Lenses were dissected and photographed using a SZX16 dissecting microscope equipped with a digital camera (Olympus). Lens diameters were measured and used to calculate lens volume, assuming a spherical shape.

Measurement of lens intracellular hydrostatic pressure. Intracellular hydrostatic pressures were measured as previously described (19). Briefly, microelectrode resistance (1.5–2.0 MΩ when filled with 3 M KCl) was recorded in solution outside of the lens by injecting serial current pulses and recording the amplitudes of the responding voltage steps to determine the resistance of the tip of the electrode. After the electrode was inserted into the lens, positive intracellular pressure pushed cytoplasm into the tip, causing the resistance to increase. A side port on the electrode holder connected to a mercury manometer allowed adjustment of the pressure within the electrode. The pressure within the electrode was increased to push cytoplasm back into the fiber cell. When the amplitude of the electrode resistance returned to its original value measured in the bathing solution, pressure within the electrode was equal to intracellular pressure, and this value was recorded. Intracellular pressures were recorded at different depths within each lens along a track between the surface and center 45° between the posterior pole and equator. In some experiments, the pressure-sensing electrode was maintained at a constant position near the lens surface, and serial pressure measurements were made every 5–10 minutes while the lens was incubated with 10 μM AKT inhibitor VIII (EMD Millipore) and/or 0.2 mM strophanthidin (Sigma-Aldrich). 0.2 mM strophanthidin was chosen as a half-saturating concentration of inhibitor for mouse Na^+/K^+-ATPase based on species variation in sensitivity (46, 47).

Measurement of lens intracellular sodium. Intracellular sodium concentration was measured using a dual-wavelength spectrometer system as previously described (27). Sodium-binding benzofuran isophthalate (SBFI; 0.2 mM) was injected into fiber cells at different depths in the lens by advancing a microelectrode along a track between the surface and center 45° between the posterior pole and equator. The ratios of emission at 360/380 nm excitation were compared with sodium calibration curves that were determined as previously described for intracellular calcium (28).

Measurement of lens epithelial cell Na^+/K^+-ATPase activity. Lens epithelial cells were dissociated by incubation of dissected capsules with 0.25% trypsin for 5–7 minutes at 37°C. Na^+/K^+-ATPase currents were measured as previously described (48), with the exception that 5 mM strophanthidin (Sigma-Aldrich) was used as an inhibitor instead of dihydro-ouabain. 5 mM strophanthidin was chosen as a saturating concentration of inhibitor for mouse Na^+/K^+-ATPase based on species variation in sensitivity (46, 47). Briefly, isolated lens epithelial cells were placed in a chamber in which the perfusion solution could be exchanged. Individual cells were subjected to whole-cell patch clamp using an Axopatch 1B amplifier (Axon Instruments), and membrane capacitance was determined in current clamp mode. To measure the Na^+/K^+-ATPase current, cells were perfused with 5 mM strophanthidin while voltage was clamped at 0 mV. The change in membrane current due to superfusion of strophanthidin was recorded to provide a direct measure of Na^+/K^+-ATPase activity, then divided by the cell capacitance to determine the current density. In some experiments, epithelial cells were incubated in the presence of 5 μM AKT inhibitor VIII (EMD Millipore) for 30 minutes prior to measurement of the Na^+/K^+-ATPase current.

Western blotting. Lenses were dissected from eyes and transferred to calcium- and magnesium-free PBS. The lens capsule was then peeled away from the fiber cell mass using fine forceps. For Western blotting, capsules were transferred to 2× sample buffer, separated on SDS-PAGE gels, and transferred to nitrocellulose membranes. Blots were probed with rabbit monoclonal antibodies against PTEN and mouse monoclonal antibodies against serine 473 phospho-AKT (Cell Signaling Technology), or with rabbit polyclonal antibodies against the α subunit of the Na^+/K^+-ATPase and total AKT1/2/3 (Santa Cruz Biotechnology). Peroxidase-conjugated goat anti-rabbit (Jackson ImmunoResearch) or sheep anti-mouse (GE Healthcare) secondary antibodies were used prior to ECL detection. In some experiments, dissected lenses were incubated in the presence of 5 μM AKT inhibitor VIII for 30 minutes prior to lens capsule dissection. Band densities from 4 independent blots were quantified using ImageJ (49).

Histology. Mouse eyes were dissected and fixed in a 4% formaldehyde solution in PBS for 16–24 hours at room temperature. In some experiments, pregnant female mice were injected intraperitoneally with AKT inhibitor V (Calbiochem) dissolved in 2% DMSO at 1 mg/kg/d on E16.5, E17.5, and E18.5 (31). Between birth and P7, eyes were dissected and fixed. Fixed eyes were rinsed with PBS, dehydrated through an ethanol series, and embedded in paraffin. Sections of 2–3 μm were cut on a diamond knife, deparaffinized, and stained with H&E. Histological sections were viewed on a BX51 microscope and photographed with a DP72 digital camera (Olympus).

Statistics. Data are presented as mean ± SD. Statistical significance was determined using 1-way ANOVA or 2-tailed Student's *t* test. A *P* value less than 0.05 was considered significant.

Study approval. Animal studies were approved by the IACUC of Stony Brook University.

Acknowledgments

This work was supported by NIH grants EY012995 (to M.L. Robinson), DK062722 (to R.Z. Lin), EY006391 (to R.T. Mathias), and EY013163 (to T.W. White).

Received for publication April 11, 2013, and accepted in revised form September 12, 2013.

Address correspondence to: Thomas W. White, Department of Physiology and Biophysics, Stony Brook University, T5-147, Basic Science Tower, Stony Brook, New York 11794-8661, USA. Phone: 631.444.9683; Fax: 631.444.3432; E-mail: thomas.white@stonybrook.edu.

1. Hollander MC, Blumenthal GM, Dennis PA. PTEN loss in the continuum of common cancers, rare syndromes and mouse models. *Nat Rev Cancer*. 2011;11(4):289–301.
2. Lloyd KM, Dennis M. Cowden's disease. A possible new symptom complex with multiple system involvement. *Ann Intern Med*. 1963;58:136–142.
3. Uppal S, Mistry D, Coatesworth AP. Cowden disease: a review. *Int J Clin Pract*. 2007;61(4):645–652.
4. Starink TM. Cowden's disease: analysis of fourteen new cases. *J Am Acad Dermatol*. 1984;11(6):1127–1141.
5. Boccone L, Dessi V, Serra G, Zibordi F, Loudianos G. Bannayan-Riley-Ruvalcaba syndrome with posterior subcapsular congenital cataract and a consensus sequence splicing PTEN mutation. *Am J Med Genet A*. 2008;146A(2):257–260.
6. Marchese C, et al. Granular cell tumor in a PHTS patient with a novel germline PTEN mutation. *Am J Med Genet A*. 2003;120A(2):286–288.
7. Trumler AA. Evaluation of pediatric cataracts and systemic disorders. *Curr Opin Ophthalmol*. 2011;22(5):365–379.
8. Di Cristofano A, Pesce B, Cordon-Cardo C, Pandolfi PP. Pten is essential for embryonic development and tumour suppression. *Nat Genet*. 1998; 19(4):348–355.
9. Cantley LC, Neel BG. New insights into tumor suppression: PTEN suppresses tumor formation by restraining the phosphoinositide 3-kinase/AKT pathway. *Proc Natl Acad Sci U S A*. 1999;96(8):4240–4245.
10. Waite KA, Eng C. Protean PTEN: form and function. *Am J Hum Genet*. 2002;70(4):829–844.
11. Ilic N, Roberts TM. Comparing the roles of the p110alpha and p110beta isoforms of PI3K in signaling and cancer. *Curr Top Microbiol Immunol*. 2010;347:55–77.
12. Cantley LC. The phosphoinositide 3-kinase pathway. *Science*. 2002;296(5573):1655–1657.
13. Sarbassov DD, Ali SM, Sabatini DM. Growing roles for the mTOR pathway. *Curr Opin Cell Biol*. 2005;17(6):596–603.
14. Martinez G, de Iongh RU. The lens epithelium in ocular health and disease. *Int J Biochem Cell Biol*. 2010;42(12):1945–1963.
15. Donaldson P, Kistler J, Mathias RT. Molecular solutions to mammalian lens transparency. *News Physiol Sci*. 2001;16:118–123.
16. Candia OA, Zamudio AC. Regional distribution of the Na(+) and K(+) currents around the crystalline lens of rabbit. *Am J Physiol Cell Physiol*. 2002;282(2):C252–C262.
17. Mathias RT, White TW, Gong X. Lens gap junctions in growth, differentiation, and homeostasis. *Physiol Rev*. 2010;90(1):179–206.
18. Tamiya S, Dean WL, Paterson CA, Delamere NA. Regional distribution of Na,K-ATPase activity in porcine lens epithelium. *Invest Ophthalmol Vis Sci*. 2003;44(10):4395–4399.
19. Gao J, Sun X, Moore LC, White TW, Brink PR, Mathias RT. Lens intracellular hydrostatic pressure is generated by the circulation of sodium and modulated by gap junction coupling. *J Gen Physiol*. 2011;137(6):507–520.
20. Donaldson PJ, Musil LS, Mathias RT. Point: A critical appraisal of the lens circulation model — an experimental paradigm for understanding the maintenance of lens transparency? *Invest Ophthalmol Vis Sci*. 2010;51(5):2303–2306.
21. Candia OA, Mathias R, Gerometta R. Fluid circulation determined in the isolated bovine lens. *Invest Ophthalmol Vis Sci*. 2012;53(11):7087–7096.
22. Shiels A, Bennett TM, Hejtmancik JF. Cat-Map: putting cataract on the map. *Mol Vis*. 2010;16:2007–2015.
23. Sachs E, Larsen RL. Cancer and the lens. *Am J Ophthalmol*. 1948;31(5):561–564.
24. Suzuki A, et al. T cell-specific loss of Pten leads to defects in central and peripheral tolerance. *Immunity*. 2001;14(5):523–534.
25. Zhao H, Yang Y, Rizo CM, Overbeek PA, Robinson ML. Insertion of a Pax6 consensus binding site into the alphaA-crystallin promoter acts as a lens epithelial cell enhancer in transgenic mice. *Invest Ophthalmol Vis Sci*. 2004;45(6):1930–1939.
26. Gao J, Sun X, Moore LC, Brink PR, White TW, Mathias RT. The effect of size and species on lens intracellular hydrostatic pressure. *Invest Ophthalmol Vis Sci*. 2013;54(1):183–192.
27. Wang H, et al. The effects of GPX-1 knockout on membrane transport and intracellular homeostasis in the lens. *J Membr Biol*. 2009;227(1):25–37.
28. Gao J, Sun X, Martinez-Wittinghan FJ, Gong X, White TW, Mathias RT. Connections between connexins, calcium, and cataracts in the lens. *J Gen Physiol*. 2004;124(4):289–300.
29. Ballou LM, Selinger ES, Choi JY, Drueckhammer DG, Lin RZ. Inhibition of mammalian target of rapamycin signaling by 2-(morpholin-1-yl) pyrimido[2,1-α]isoquinolin-4-one. *J Biol Chem*. 2007;282(33):24463–24470.
30. Pau H. Cortical and subcapsular cataracts: significance of physical forces. *Ophthalmologica*. 2006;220(1):1–5.
31. Puig I, Champeval D, De Santa Barbara P, Jaubert F, Lyonnet S, Larue L. Deletion of Pten in the mouse enteric nervous system induces ganglioneuromatosis and mimics intestinal pseudoobstruction. *J Clin Invest*. 2009;119(12):3586–3596.
32. Lindhurst MJ, et al. A mosaic activating mutation in AKT1 associated with the Proteus syndrome. *N Engl J Med*. 2011;365(7):611–619.
33. Sheard RM, Pope FM, Snead MP. A novel ophthalmic presentation of the Proteus syndrome. *Ophthalmology*. 2002;109(6):1192–1195.
34. Boswell BA, Lein PJ, Musil LS. Cross-talk between fibroblast growth factor and bone morphogenetic proteins regulates gap junction-mediated intercellular communication in lens cells. *Mol Biol Cell*. 2008;19(6):2631–2641.
35. Le AC, Musil LS. A novel role for FGF and extracellular signal-regulated kinase in gap junction-mediated intercellular communication in the lens. *J Cell Biol*. 2001;154(1):197–216.
36. Shakespeare TI, et al. Interaction between Connexin50 and mitogen-activated protein kinase signaling in lens homeostasis. *Mol Biol Cell*. 2009; 20(10):2582–2592.
37. Delamere NA, Tamiya S. Lens ion transport: from basic concepts to regulation of Na,K-ATPase activity. *Exp Eye Res*. 2009;88(2):140–143.
38. Delamere NA, Tamiya S. Expression, regulation and function of Na,K-ATPase in the lens. *Prog Retin Eye Res*. 2004;23(6):593–615.
39. Mandal A, Shahidullah M, Beimgraben C, Delamere NA. The effect of endothelin-1 on Src-family tyrosine kinases and Na,K-ATPase activity in porcine lens epithelium. *J Cell Physiol*. 2011; 226(10):2555–2561.
40. Shahidullah M, Mandal A, Beimgraben C, Delamere NA. Hyposmotic stress causes ATP release and stimulates Na,K-ATPase activity in porcine lens. *J Cell Physiol*. 2012;227(4):1428–1437.
41. Lu Z, et al. Suppression of phosphoinositide 3-kinase signaling and alteration of multiple ion currents in drug-induced long QT syndrome. *Sci Transl Med*. 2012;4(131):131ra150.
42. Wan X, et al. Oxidative inactivation of the lipid phosphatase phosphatase and tensin homolog on chromosome ten (PTEN) as a novel mechanism of acquired long QT syndrome. *J Biol Chem*. 2011;286(4):2843–2852.
43. Takeuchi K, Gertner MJ, Zhou J, Parada LF, Bennett MV, Zukin RS. Dysregulation of synaptic plasticity precedes appearance of morphological defects in a Pten conditional knockout mouse model of autism. *Proc Natl Acad Sci U S A*. 2013; 110(12):4738–4743.
44. Weston MC, Chen H, Swann JW. Multiple roles for mammalian target of rapamycin signaling in both glutamatergic and GABAergic synaptic transmission. *J Neurosci*. 2012;32(33):11441–11452.
45. DeRosa AM, et al. The cataract causing Cx50-S50P mutant inhibits Cx43 and intercellular communication in the lens epithelium. *Exp Cell Res*. 2009;315(6):1063–1075.
46. Abeywardena MY, McMurchie EJ, Russell GR, Charnock JS. Species variation in the ouabain sensitivity of cardiac Na^+/K^+-ATPase. A possible role for membrane lipids. *Biochem Pharmacol*. 1984;33(22):3649–3654.
47. Garner MH. Na,K-ATPases of the lens epithelium and fiber cell: formation of catalytic cycle intermediates and Na+: K+ exchange. *Exp Eye Res*. 1994;58(6):705–718.
48. Gao J, Sun X, Yatsula V, Wymore RS, Mathias RT. Isoform-specific function and distribution of Na/K pumps in the frog lens epithelium. *J Membr Biol*. 2000;178(2):89–101.
49. Schneider CA, Rasband WS, Eliceiri KW. NIH Image to ImageJ: 25 years of image analysis. *Nat Methods*. 2012;9(7):671–675.